Nitsche-type Mortaring for Maxwell's Equations

K. Hollaus[1], **D. Feldengut**[1], **J. Schöberl**[2], **M. Wabro**[3], **and D. Omeragic**[4]

[1]RWTH Aachen University, Germany
[2]Vienna University of Technology, Austria
[3]CST AG, Germany
[4]Schlumberger-Doll Research, USA

Abstract—

We propose a new method for treating transmission conditions on non-matching meshes. The basic method is a hybrid version of Nitsche's method. By introducing a scalar potential on the interface we obtain a robust method for the low frequency limit. In order to simplify numerical integration, we use smooth B-spline basis functions on the interface. We present the formulation for scalar potential problems and for time-harmonic Maxwell's equations. A simple well logging example is used to benchmark the algorithm.

1. INTRODUCTION

The finite element modeling can often be simplified by allowing independent meshes for different parts. Typical examples are rotating parts in electric machines, or a logging while drilling (LWD) tool moving through the bore-hole. The difficulty is an accurate discretization of the transmission conditions on the interface. Since interpolation methods lose accuracy, mortar methods became popular in recent years [11, 3]. Here, the continuity of the primal field is enforced by an additional equation, and a Lagrange parameter at the interface must be added. The resulting linear system has saddle point structure. In theory, it is tricky to prove stability, and finite element spaces must be chosen carefully. In practice, it's non-trivial to implement the numerical integration over non-matching meshes, in particular for 3D applications. The Nitsche method is an alternative to the mortar method. Here, no additional Lagrange parameter comes in, and the saddle point problem can be avoided [8, 2]. The price to pay are additional boundary terms in the variational formulation. We choose a hybrid formulation with additional variables at the interface as in [6]. We propose to use smooth B-spline basis functions on the interface to simplify numerical integration.

2. THE POISSON EQUATION

We decompose the domain Ω into non-overlapping sub-domains Ω_1 and Ω_2, and call the common interface γ. For introducing the method, we start with the Dirichlet problem for the Poisson equation

$$\begin{aligned} -\Delta u &= f \qquad \text{in } \Omega_1 \cup \Omega_2, \\ u &= 0 \qquad \text{on } \partial\Omega, \end{aligned}$$

and the transmission conditions

$$u_{|\Omega_1} = u_{|\Omega_2}, \tag{1}$$

$$\frac{\partial u}{\partial n_1}_{|\Omega_1} = -\frac{\partial u}{\partial n_2}_{|\Omega_2} \qquad \text{on } \gamma. \tag{2}$$

The idea of the Nitsche method is to multiply by test-functions v, and integrate by parts on the sub-domains:

$$\int_{\Omega_i} \nabla u \cdot \nabla v - \int_{\partial\Omega_i} \frac{\partial u}{\partial n} v = \int_{\Omega_i} f v \qquad \text{for } i \in \{1, 2\}$$

Next, we introduce an additional independent variable λ on the interface, which shall be the restriction of $u_1 = u_2$ on the interface. We define the function spaces

$$\begin{aligned} V &:= \{v \in H^1(\Omega_1) \times H^1(\Omega_2) : v = 0 \text{ on } \partial\Omega\}, \\ W &:= \{\mu \in L_2(\partial\Omega_1 \cup \partial\Omega_2) : \mu = 0 \text{ on } \partial\Omega). \end{aligned}$$

Note that functions form V are piece-wise in H^1, but may be discontinuous across the interface. Functions in W are single-valued on the interface. The solution (u, λ) satisfies the variational equation: find $u \in V$ and $\lambda \in W$ such that

$$\sum_{i=1}^{2} \Big\{ \int_{\Omega_i} \nabla u \cdot \nabla v - \int_{\partial\Omega_i} \frac{\partial u}{\partial n}(v-\mu) - \int_{\partial\Omega_i} \frac{\partial v}{\partial n}(u-\lambda) + \frac{\alpha p^2}{h} \int_{\partial\Omega_i} (u-\lambda)(v-\mu) \Big\} = \int_\Omega fv$$

for $v \in V$ and $\mu \in W$. For the true solution the terms involving $u - \lambda$ vanish. Furthermore, $\sum_i \int_{\partial\Omega_i} \frac{\partial u}{\partial n}\mu$ cancel due to the transmission condition (2) and the essential boundary condition on the test function μ.

The left hand side defines the bilinear-form $A(.,.)$, which depends on the chosen finite element space. Here, p denotes the polynomial degree, and h is the mesh size. The parameter α must be chosen sufficiently large, and is typically set as $\alpha = 10$. The bilinear-form is symmetric and coercive with respect to the norm defined by

$$|\!|\!|(u,\lambda)|\!|\!|^2 = \sum_{i=1}^{2} \Big\{ \|\nabla u\|^2_{\Omega_i} + \frac{p^2}{h} \|u-\lambda\|^2_{\partial\Omega_i} \Big\}.$$

The key to prove coercivity is to bound the mixed term by the diagonal terms, i.e., the inequality

$$\sum_{i=1}^{2} \int_{\partial\Omega_i} \frac{\partial u}{\partial n}(v-\mu) \le c(|\!|\!|(u,\lambda)|\!|\!|^2 + |\!|\!|(v,\mu)|\!|\!|^2)$$

on the finite element space. This is standard in discontinuous Galerkin methods [1].

The formulation allows to use independent meshes in both sub-domains, and another discrete space on the interface. It requires to integrate basis functions on the boundary of the domain meshes against basis functions defined on an interface mesh. Gauss integration rules are exact for piecewise polynomials on the mesh, but converge very slowly if the interface functions are not smooth or even not continuous. Then an intersection mesh should be used. But, this is difficult to generate, in particular for curved 3D domains. We propose a different strategy: Since the interface domain is often simple, e.g., a cylinder, we can use a structured mesh and high order B-spline basis functions [5]. The use of Gauss integration on the boundary mesh is not exact, but still of high order for the smooth basis functions on the interface.

3. MAXWELL'S EQUATIONS

We consider the time harmonic Maxwell's equations in vector potential formulation

$$\operatorname{curl} \mu^{-1} \operatorname{curl} u + \kappa u = j \qquad \text{in } \Omega_i, \tag{3}$$

with $\kappa = i\omega\sigma - \omega^2\epsilon$, and

$$E = -i\omega u, \quad H = \mu^{-1} \operatorname{curl} u.$$

The transmission conditions for the tangential components of the electric and magnetic field are

$$\begin{aligned} u_1 \times n_1 &= -u_2 \times n_2, \\ \mu_1^{-1} \operatorname{curl} u_1 \times n_1 &= -\mu_2^{-1} \operatorname{curl} u_2 \times n_2. \end{aligned}$$

Proceeding as in the scalar case, one obtains

$$\int_{\Omega_i} \{\mu^{-1} \operatorname{curl} u \cdot \operatorname{curl} v + \kappa u \cdot v\} + \int_{\partial\Omega_i} \mu^{-1} \operatorname{curl} u \cdot (v \times n) = \int_{\Omega_i} j \cdot v \tag{4}$$

and the variational formulation: find (u, λ) such that

$$\begin{aligned} \sum_{i=1}^{2} \Big\{ & \int_{\Omega_i} \mu^{-1} \{\operatorname{curl} u \cdot \operatorname{curl} v + \kappa u \cdot v\} + \int_{\partial\Omega_i} \mu^{-1} \operatorname{curl} u \cdot [(v-\mu) \times n] + \\ & \int_{\partial\Omega_i} \mu^{-1} \operatorname{curl} v \cdot [(u-\lambda) \times n] + \frac{\alpha p^2}{\mu h} \int_{\partial\Omega_i} [(u-\lambda) \times n] \cdot [(v-\mu) \times n] \Big\} \;=\; \int_\Omega j \cdot v, \end{aligned}$$

where $u, v \in H(\mathrm{curl}, \Omega_1) \times H(\mathrm{curl}, \Omega_2)$, and λ, μ are tangential vector valued fields on the interface. For simplification let us assume $\kappa \in \mathbb{R}^+$ and small. Then, the bilinear-form is coercive with respect to the norm

$$|\!|\!|(u,\lambda)|\!|\!|^2 = \sum_{i=1}^{2} \Big\{ \mu^{-1} \| \operatorname{curl} u \|^2_{\Omega_i} + \kappa \|u\|^2_{\Omega_i} + \frac{p^2}{\mu h} \|(u-\lambda)\times n\|^2_{\partial\Omega_i} \Big\}.$$

An important point for discretizing low frequency problems with small κ is to treat the gradient sub-space. Let $u = \nabla\phi$; the energy norm of u should scale as

$$\|u\|^2 = \mu^{-1} \| \operatorname{curl} u\|^2 + \kappa \|u\|^2 = \kappa \|\nabla\phi\|^2 = O(\kappa).$$

But, the penalty term $\|(u-\lambda)\times n\|$ scales like $O(1)$ and thus is an over-penalization for gradient fields. The goal is now to modify the formulation to have separate penalization terms for gradient and rotational components.

First, we derive a relation for scalar test functions on the boundary. Set $v = \nabla\psi$ in (4) and obtain

$$\int_{\Omega_i} \kappa u \cdot \nabla\psi + \int_{\partial\Omega_i} \mu^{-1} \operatorname{curl} u \cdot (\nabla\psi \times n) = \int_{\Omega} j \cdot \nabla\psi. \tag{5}$$

Apply the div operator on the sub-domains Ω_i to equation (3), and test by ψ to obtain

$$\int_{\Omega_i} \operatorname{div}(\kappa u)\, \psi = \int_{\Omega_i} \operatorname{div} j\, \psi.$$

Integration by parts on the sub-domains leads to

$$-\int_{\Omega_i} \kappa u \cdot \nabla\psi + \int_{\partial\Omega_i} \kappa u_n \psi = -\int_{\Omega_i} j \cdot \nabla\psi + \int_{\partial\Omega_i} j_n \psi \tag{6}$$

Adding equations (5) and (6) we obtain

$$\sum_{i=1}^{2} \left\{ \int_{\partial\Omega_i} \mu^{-1} \operatorname{curl} u \cdot (\nabla\psi \times n) + \int_{\partial\Omega_i} \kappa u_n \psi \right\} = \sum_{i=1}^{2} \int_{\partial\Omega_i} j_n \psi \tag{7}$$

Note that ψ is evaluated only on the boundary of the sub-domains Ω_i, and thus it is enough to define ψ only on the boundary.

We introduce a new scalar field variable $\phi_\gamma \in W$ on the interface, which shall be the scalar potential of a Helmholtz-type decomposition of u on the interface. We set $\phi_i = \phi_{\gamma|\partial\Omega_i}$ on the sub-domain boundaries. Instead of posing continuity for $u \times n$, we pose it for $(u - \nabla\phi) \times n$ and ϕ separately. This allows different scalings for the gradient part and the rotational part. In a first step, we redefine the interface vector variable as the rotational part, i.e., $\lambda \times n = (u - \nabla\phi) \times n$, and add a penalty term also for $\phi = \phi_\gamma$:

$$\begin{aligned} \sum_{i=1}^{2} \Bigg\{ & \int_{\Omega_i} \{\mu^{-1} \operatorname{curl} u \cdot \operatorname{curl} v + \kappa u v\} + \int_{\partial\Omega_i} \mu^{-1} \operatorname{curl} u\, [(v-\mu)\times n] + \\ & \int_{\partial\Omega_i} \mu^{-1} \operatorname{curl} v\, [(u - \nabla\phi - \lambda)\times n] + \frac{\alpha p^2}{\mu h} \int_{\partial\Omega_i} [(u-\nabla\phi-\lambda)\times n][(v-\nabla\psi-\mu)\times n] + \\ & \frac{\alpha p^2}{h} \int_{\partial\Omega_i} \kappa(\phi-\phi_\gamma)(\psi-\psi_\gamma) \Bigg\} \quad = \quad \int_{\Omega} j v \end{aligned}$$

The skew terms do not lead to a symmetric bilinear-form. Now, we subtract relation (7), and use

$\kappa u_n - j_n$ continuous following from the transmission conditions to obtain

$$\sum_{i=1}^{2}\Bigg\{\int_{\Omega_i}\{\mu^{-1}\operatorname{curl} u\cdot\operatorname{curl} v+\kappa uv\}+\int_{\partial\Omega_i}\mu^{-1}\operatorname{curl} u\,[(v-\nabla\psi-\mu)\times n]+$$
$$\int_{\partial\Omega_i}\mu^{-1}\operatorname{curl} v\,[(u-\nabla\phi-\lambda)\times n]+\frac{\alpha p^2}{\mu h}\int_{\partial\Omega_i}[(u-\nabla\phi-\lambda)\times n][(v-\nabla\psi-\mu)\times n]+$$
$$-\int_{\partial\Omega_i}\kappa u_n(\psi-\psi_\gamma)-\int_{\partial\Omega_i}\kappa v_n(\phi-\phi_\gamma)+\frac{\alpha p^2}{h}\int_{\partial\Omega_i}\kappa(\phi-\phi_\gamma)(\psi-\psi_\gamma)\Bigg\}=$$
$$\sum_{i=1}^{2}\Bigg\{\int_{\Omega_i}jv-\int_{\partial\Omega_i}j_n\psi\Bigg\}$$

As in the scalar case, one can easily show coercivity on the finite element space with respect to the semi-norm

$$|\!|\!|(u,\lambda,\phi,\phi_\gamma)|\!|\!|^2:=\sum_{i=1}^{2}\Bigg\{\mu^{-1}\|\operatorname{curl} u\|^2_{\Omega_i}+\kappa\|u\|^2_{\Omega_i}+\frac{p^2}{\mu h}\|(u-\nabla\phi-\lambda)\times n\|^2_{\partial\Omega_i}+\frac{\kappa p^2}{h}\|\phi-\phi_\gamma\|^2_{\partial\Omega_i}\Bigg\}.$$

Now, the penalization of the gradient field ϕ is of order κ, and only the rotational part $u-\nabla\phi$ is penalized of order 1.

We propose to discretize u by Nedelec finite elements [7] of order p, ϕ by continuous, scalar finite elements of order $p+1$ on $\partial\Omega_i$, ϕ_γ by tensor product B-splines of order m, and λ by Nedelec-type B-splines satisfying an exact sequence [4]. The full finite element error analysis fill be given in a subsequent paper.

4. A NUMERICAL EXAMPLE

To demonstrate the feasibility of the proposed method the simplified logging-while-drilling (LWD) tool shown in Fig.1 has been analyzed numerically. Two identical conducting loops, i.e. a sending and a receiving antenna, represent the sensor. In general several finite element meshes might be created of both the sensor and the surrounding mud and formation to simulate the LWD tool in use. The present formulation avoids repeated complete modeling of all domains by means of separate non matching meshes which can be merged together with the Nitsche method.

Although the geometry of the problem is rotational symmetric, the problem was modeled in 3D. All dimension are given in inches. The transmitter-receiver spacing is 46", and the operating frequency ranges from 20 kHz to 2.0 MHz. The electric conductivities of the tool body, the borehole mud and the formation have been selected with $1.0\cdot10^6$ S/m, 1.0 S/m and 0.01 S/m, respectively. A releative electric permittivity of $\varepsilon_r = 26.67$ for 2MHz has been considered for the borehole mud and the formation. The releative electric permittivity was determined with $\varepsilon_r = 38.63$ for 400kHz and all smaller frequencies. The relative permeability was chosen with $\mu_r = 1.0$ throughout the problem region. Due to the high conductivity of the tool body, it has been eliminated in the model by using a proper surface impedance boundary condition. The transmitter is excited by an electric current of 1.0 A, and the induced voltage in the receiver is computed.

For that, we have performed computations with first and second order Nédélec elements of the second type, see Table 1 and Table 2. Once we used a standard method with a conforming mesh across the interface. Then we used the proposed Nitsche method, with 5 B-splines of order 5 in azimuthal direction, and 150 B-splines of order 5 in axial direction. We can observe that the difference between the standard method and the Nitsche method is much less than the difference between first and second order elements. We conclude that the error due to the proposed Nitsche method is small for LWD tool simulations of this type.

5. CONCLUSION

We have developed domain decomposition techniques based on Nitsche's method to discretize transmission conditions on non-matching meshes. Due to the use of a scalar potential on the interface, the method is robust at low frequencies. The algorithm was tested on a simple well logging application, where independent meshes for the tool-borehole volume and the formation were used.

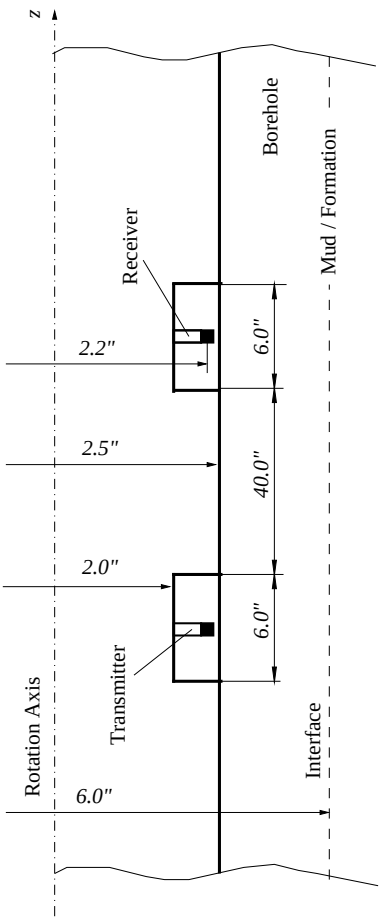

Figure 1: Sketch of the LWD tool (rotated) with dimensions in inches.

frequency [kHz]	standard, rec volt [nV] 185 810 dofs	Nitsche, rec volt [nV] 195 383 dofs
20	$25.44 - i\,18.38$	$25.43 - i\,18.37$
100	$71.68 - i\,197.5$	$71.65 - i\,197.3$
400	$124.9 - i\,963.0$	$124.9 - i\,962.3$
2000	$-635.9 - i\,5295$	$-634.8 - i\,5255$

Table 1: Numerical results for first order elements.

frequency [kHz]	standard, rec volt [nV] 733 881 dofs	Nitsche, rec volt [nV] 736 939 dofs
20	$24.99 - i\,18.47$	$24.98 - i\,18.47$
100	$70.25 - i\,196.7$	$70.23 - i\,196.7$
400	$121.7 - i\,957.9$	$121.7 - i\,957.7$
2000	$-648.1 - i\,5256$	$-647.9 - i\,5255$

Table 2: Numerical results for second order elements.

ACKNOWLEDGMENT

The first three authors would like to thank Schlumberger Technology corporation for financial support of this work. The authors are especially grateful to colleagues in Schlumberger Research and Technology Centers for their help and many useful discussion and suggestions during the course of this work.

REFERENCES

1. Arnold, D. N., F. Brezzi, B. Cockburn, and D. Marini, "Unified analysis of discontinuous Galerkin methods for elliptic problems," *SIAM J. Numer. Anal*, Vol. 39, No. 5, 1749–1779, 2002.
2. Becker, R, P. Hansbo and R. Stenberg, "A finite element method for domain decomposition with non-matching grids," *M2AN Math. Model. Numer. Anal.*, Vol. 37, No. 2, 209–225, 2003.
3. Ben Belgacem, F., A. Buffa and Y. Maday, "The mortar finite element method for 3D Maxwell equations: first results," *SIAM J. Numer. Anal*, Vol. 39, No. 3, 880-901, 2001.
4. Buffa, A., G. Sangalli and R. Vazquez, "Isogeometric analysis in electromagnetics: B-splines approximation," *Comput. Methods Appl. Mech. Engrg*, doi:10.1016/j.cma.2009.12.002.
5. de Boor, C, *A practical guide to splines. Revised edition*, Springer-Verlag, New York, 2001.
6. Egger, H., "A class of hybrid mortar finite element methods for interface problems with non-matching meshes," preprint AICES-2009-2, Aachen Institute for Advanced Study in Computational Engineering Science, 2009.
7. Nédélec, J.-C. "A new family of mixed finite elements in $\mathbb{R}^3$." *Numer. Math.*, Vol. 50, No. 1, 57-81, 1986.
8. Nitsche, J., "Über ein Variationsprinzip zur Lösung von Dirichlet-Problemen bei Verwendung von Teilrumen, die keinen Randbedingungen unterworfen sind.", Abh. Math. Sem. Univ. Hambug Vol. 36, 915., 1971.
9. Omeragic, D, "EM modeling of logging-while drilling resistivity tool responses: State of art and challenges," in *Proceedings of Mathematics of finite elements and application (MAFELAP) Conference 2003*, Brunel University, Uxbridge, June 2003.
10. Pardo, D., M. J. Nam, C. Torres-Verdin and M. Paszynski, "A Parallel, Fourier Finite-Element Formulation with an Iterative Solver for the Simulation of 3D LWD Measurements Acquired in Deviated Wells," *PIERS Online*, Vol. 4, No. 5, 551–555, 2008.
11. Wohlmuth, B., "A mortar finite element method using dual spaces for the Lagrange multiplier," SIAM J. Numer. Anal, Vol. 38, No. 3, 989–1012, 2000.